Title: Synthesis, chemical characterization, and mu-opioid receptor activity assessment of the emerging group of “nitazene” 2-benzylbenzimidazole synthetic opioids.

Authors: Vandeputte, M., Van Uytfanghe, K., Layle, N., St Germaine, D., Iula, D., & Stove, C.

In: *ACS CHEMICAL NEUROSCIENCE*, *12*(7), 1241–1251, 2021

Synthesis, Chemical Characterization, and μ-Opioid Receptor Activity Assessment of the Emerging Group of 'Nitazene' 2-Benzylbenzimidazole Synthetic Opioids

Marthe M. Vandeputte[1], Katleen Van Uytfanghe[1], Nathan K. Layle[2], Danielle M. St. Germaine[2], Donna M. Iula[2], Christophe P. Stove[1,*]

[1] Laboratory of Toxicology, Department of Bioanalysis, Faculty of Pharmaceutical Sciences, Ghent University, Ghent, Belgium

[2] Forensic Chemistry Division, Cayman Chemical Company, Ann Arbor, Michigan, USA

* Corresponding author: Christophe P. Stove (christophe.stove@ugent.be)

Abstract

Several 2-benzylbenzimidazole opioids (also referred to as 'nitazenes') recently emerged on the illicit market. The most frequently encountered member, isotonitazene, has been identified in multiple fatalities since its appearance in 2019. Although recent scheduling efforts targeted isotonitazene, many other analogues remain unregulated. Being structurally unrelated to fentanyl, little is known about the harm potential of these compounds. In this study, ten nitazenes and four metabolites were synthesized, analytically characterized via four different techniques, and pharmacologically evaluated using two cell-based β-arrestin2/mini-Gi recruitment assays monitoring μ-opioid receptor (MOR) activation. Based on absorption spectra and retention times, high-performance liquid chromatography coupled to diode-array detection (HPLC-DAD) allowed differentiation between most analogues. Time-of-flight mass spectrometry (LC-QTOF-MS) identified a fragment with *m/z* 100.11 for 12/14 compounds, which could serve as a basis for MS-based nitazene screening. MOR activity determination confirmed that nitazenes are generally highly active, with potencies and efficacies of several analogues exceeding that of fentanyl. Particularly relevant is the unexpected very high potency of the *N*-desethyl-isotonitazene metabolite, rivalling the potency of etonitazene and exceeding that of isotonitazene itself. Supported by its identification in fatalities, this likely has *in vivo* consequences. These results improve our understanding of this emerging group of opioids by laying out an analytical framework for their detection, as well as providing important new insights into their MOR activation potential.

Keywords (6)

New psychoactive substances (NPS), 2-benzylbenzimidazoles, nitazenes, μ-opioid receptor (MOR) activation, synthesis, chemical characterization

Introduction

For several years, the presence of new synthetic opioids on the illicit drug market has been increasing.[1,2] Close to 80 synthetic opioids have been detected since 2009.[2] While these compounds represent a smaller share of the total portfolio of new psychoactive substances (NPS),[1] the highly potent nature of many of these compounds poses a very high risk of poisoning.[3] In addition, as with many NPS, the opioid market is diversifying relentlessly, with high potency opioids continuously (re-)appearing. Between 2008 and 2018, newly identified opioid NPS mainly encompassed fentanyl derivatives, which are now increasingly controlled.[4–6] As a result, the balance recently tipped towards non-fentanyl analogues.[2,3] In many cases, the synthesis of these newly abused synthetic opioids can be traced back to early research articles exploring their potential as novel opioid analgesics. However, due to side effects and addiction liability, most compounds were never marketed.[2] Nowadays, chemists involved in the manufacturing of NPS increasingly find their way to these original publications in search of new drugs to diversify the recreational drug market and continuously evade legislation. Recent examples include the emergence of AP-237, piperidylthiambutene, brorphine and several 2-benzylbenzimidazole opioids, also referred to as nitazenes.[2,3,7–10]

Structurally unrelated to traditional opiates or (the later synthesized) fentanyl **(Fig. 1)**, the synthesis of a series of benzimidazole derivatives was first reported in the late 50s and early 60s by a Swiss company.[11–17] In mice, the antinociceptive effect of several benzimidazoles exceeded that of morphine, the antinociceptive potency of etonitazene, the most potent derivative, being a 1000-fold higher than that of morphine.[13,18] While several benzimidazole derivatives were patented,[19–21] further development was halted and no benzimidazole analgesics have ever been clinically approved.[22–24] Apart from observational animal studies (primarily tail-flick; a detailed overview of these studies is given by Ujváry *et al.*[24], a summary is also included in **S1**), there are no studies that systematically evaluated the μ-opioid receptor (MOR) activation potential of this emerging class of synthetic opioids.

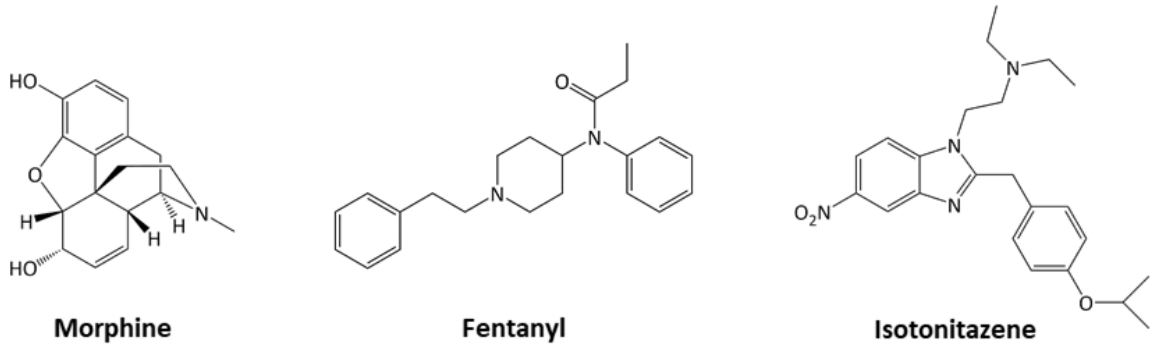

Figure 1. Structures of morphine, fentanyl, and isotonitazene. Isotonitazene, the prototypical member of the benzimidazole opioids, is structurally unrelated to traditional opiates or fentanyl.

As early as 1975, the chemist Alexander T. Shulgin warned for the potential misuse of benzimidazole opioids as heroin substitutes.[25] Apart from sporadic reports on etonitazene between 1966 and 2003,[26–30] it wasn't until quite recently that the first benzimidazoles started to emerge on drug forums and the illicit market. March 2019 marks the earliest (known) appearance of isotonitazene **(Fig. 1)**, a 5-nitro-2-benzylbenzimidazole opioid, on the drug scene in Canada and Europe.[22,31] Later that year, isotonitazene was identified in a powder sourced from an online NPS marketplace and was fully characterized,[7] generating the first report on isotonitazene since its synthesis. Following this report,

isotonitazene was formally notified to the European Monitoring Centre for Drugs and Drug Addiction (EMCDDA).[22] In the United States, isotonitazene was first found in biological samples in July 2019[32–35] and has since been identified in over 250 deaths (A. Krotulski, personal communication). The DEA issued a notice of intent to temporarily place isotonitazene in Schedule I in June 2020[36] and this went into effect August 2020. Interestingly, while this legislation also controls isotonitazene salts and (salts of) isomers, esters, and ethers,[36] only optical isomers are covered,[37] thereby currently excluding the structural isomer protonitazene. While a ban on isotonitazene has also been initiated in Europe,[38] many other nitazenes remain unscheduled worldwide. In fact, apart from clonitazene and etonitazene, which are controlled under the United Nations Single Convention on Narcotic Drugs of 1961,[39] none of the previously described 2-benzylbenzimidazole opioids are currently under (international) control.[22,24] Hence, the scheduling of isotonitazene, which has also been recommended for inclusion in Schedule I of the 1961 Convention,[40] can be anticipated to cause a dynamic shift towards the distribution and use of these non-scheduled analogues, as has been observed before for fentanyl analogues.

Recent chatter on drug fora indeed points at a renewed interest in these 'nitazene' 2-benzylbenzimidazole opioids, and their (online) availability seems to be increasing. Metonitazene, for example, was recently found in seized material in the US,[41] where its appearance seems to be growing.[42] Butonitazene, a closely related analogue, has been identified in the US[43] and Belgium (EMCDDA Early Warning System) in January-February 2021. An increasing number of desnitazenes, lacking the 5-nitro-group on the benzimidazole ring,[12] have also started to enter the drug circuit. The first of these, etodesnitazene/etazene, was very recently identified in Poland[44] and the US.[45] The known high potency and overdose risk of some nitazenes (e.g. etonitazene, isotonitazene), combined with the increasing availability in an uncontrolled setting, poses a potentially great public health threat, adding an additional layer of complexity to the ongoing opioid crisis. In addition, their presence can be easily missed in intoxication cases, as these compounds are currently not routinely screened for and may be present at very low concentrations, requiring highly sensitive analytical instrumentation for detection.[22,34] To better substantiate our knowledge on this potentially highly dangerous class of new synthetic opioids, this report focuses on the MOR activation of a set of emerging nitazenes, including three metabolites of isotonitazene and one metabolite of the highly potent etonitazene **(Fig. 2)**. In addition, advanced chemical characterization provides the first framework for improved screening of a broad panel of nitazenes.

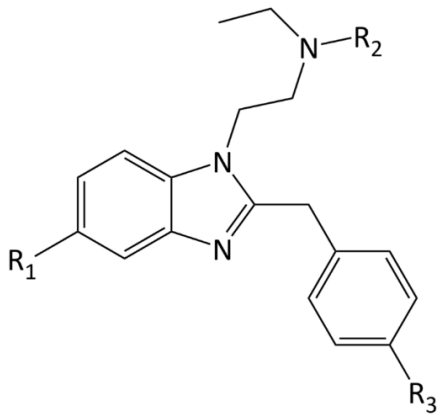

	R_1	R_2	R_3
1. **Isotonitazene**	$-NO_2$	$-C_2H_5$	$-OCH(CH_3)_2$
2. ***N*-desethyl-isotonitazene**	$-NO_2$	-H	$-OCH(CH_3)_2$
3. **4'-OH-nitazene**	$-NO_2$	$-C_2H_5$	-OH
4. **5-aminoisotonitazene**	$-NH_2$	$-C_2H_5$	$-OCH(CH_3)_2$
5. **Metonitazene**	$-NO_2$	$-C_2H_5$	$-OCH_3$
6. **Etonitazene**	$-NO_2$	$-C_2H_5$	$-OC_2H_5$
7. ***N*-desethyl-etonitazene**	$-NO_2$	-H	$-OC_2H_5$
8. **Protonitazene**	$-NO_2$	$-C_2H_5$	$-OC_3H_7$
9. **Butonitazene**	$-NO_2$	$-C_2H_5$	$-OC_4H_9$
10. **Clonitazene**	$-NO_2$	$-C_2H_5$	-Cl
11. **Flunitazene**	$-NO_2$	$-C_2H_5$	-F
12. **Isotodesnitazene**	-H	$-C_2H_5$	$-OCH(CH_3)_2$
13. **Metodesnitazene (metazene)**	-H	$-C_2H_5$	$-OCH_3$
14. **Etodesnitazene (etazene)**	-H	$-C_2H_5$	$-OC_2H_5$

Figure 2. Generic structure of the fourteen studied 'nitazene' 2-benzylbenzimidazoles. Full chemical structures are shown in **S2-S4**.

Results & Discussion

This study reports the synthesis, analytical characterization, and *in vitro* MOR activity assessment of fourteen 2-benzylbenzimidazoles (also referred to as nitazenes), a class of opioids increasingly appearing on the illicit drug market. Apart from a series of research articles exploring their potential as analgesics in the 1950s-1960s **(S1)**, the results of which are aptly discussed in a recent review by Ujváry *et al.*,[24] alarmingly little is known about these compounds and the risks associated with their use. With a focus on MOR pharmacology, this report therefore aims to address current knowledge gaps and increase public awareness of these newly emerging opioids.

Benzimidazole opioids can be synthesized via different pathways readily described in literature.[11–13,19,20,46–50] While it is not clear which route(s) are used for their illicit manufacture, several methods are simple and cost-efficient, not requiring regulated precursors.[22,24] For this report, we applied a relatively simple generic route **(Fig. 3)**.[46,48] For analogues **(1-14**, excl. **2**, **4** and **7)**, an appropriately substituted nitrobenzene **(I)** was reacted with *N,N*-diethylethylenediamine to afford synthetic intermediate **II**. The nitro group that is *ortho* to the amino group of intermediate **II** was then selectively reduced using aqueous ammonium sulfide (or a suitable equivalent) in refluxing ethanol to afford **III** (Zinin reduction).[51] Condensation of **III** with an appropriately substituted phenylacetic acid derivative (such as in the presence of *N*-ethoxycarbonyl-2-ethoxy-1,2-dihydroquinoline) afforded the desired benzimidazoles as free bases.[46] Hydrochloric or citric acid was used to convert some of the resulting benzimidazoles into their corresponding salt forms. *N*-desethyl-isotonitazene **(2)** and *N*-desethyl-etonitazene **(7)** were prepared in a similar fashion as described above, except that *N*-Boc-*N*-ethylethylenediamine was used in place of *N,N*-diethylethylenediamine in the first step of the synthesis. The Boc protecting group was carried through the subsequent steps and the final product was then treated with trifluoroacetic acid to remove the protecting group. Lastly, treatment with hydrochloric acid afforded compound **(2)** as the corresponding HCl salt. 5-aminoisotonitazene **(4)** was prepared by treating isotonitazene **(1)** under standard hydrogenation conditions to reduce the nitro group to the corresponding primary amine.

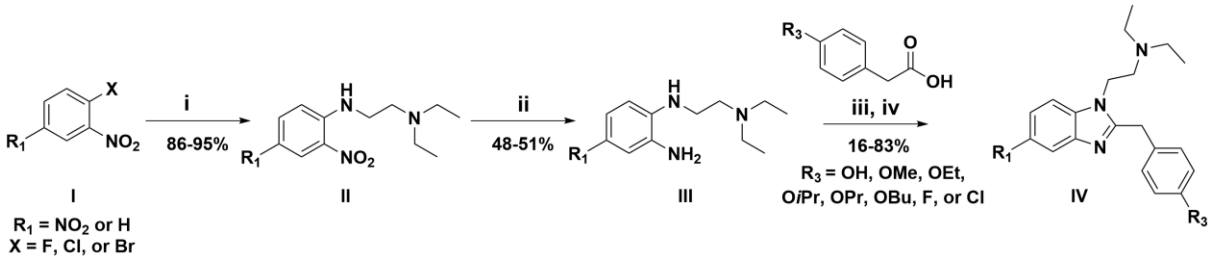

Figure 3. General scheme depicting the synthesis of the different nitazenes included in this study **(1-14)**.[46,48] Reagents and conditions: **(i)** *N,N*-diethylethylenediamine, EtOH, reflux; **(ii)** $(NH_4)_2S$, EtOH, reflux; **(iii)** *N*-ethoxycarbonyl-2-ethoxy-1,2-dihydroquinoline, CH_2Cl_2; **(iv)** HCl for **(8), (11)** and **(13)** or citric acid for **(12)** and **(14)**. Percentages indicate the yield ranges obtained for each reaction step.

The nitazenes synthesized here were extensively characterized analytically via nuclear magnetic resonance spectroscopy (^{1}H-NMR), high-performance liquid chromatography coupled to diode-array detection (HPLC-DAD), gas chromatography mass spectrometry (GC-MS), and liquid chromatography coupled to time-of-flight MS (LC-QTOF-MS). A summary of the key findings of the analytical characterization can be found in **Table 1**. **Figure 4** provides a graphical representation of the fragments found by QTOF-MS. **S7** includes a more detailed representation of the fragmentation pathway, based on A. Weissberg *et al.,*[52] including the fragments that are obtained for etonitazene as an example. **S8-S55** contain all relevant individual chromatograms and spectra. The obtained spectra match those that were previously reported by our group for isotonitazene[7] and by other research groups.[34,44,52–54]

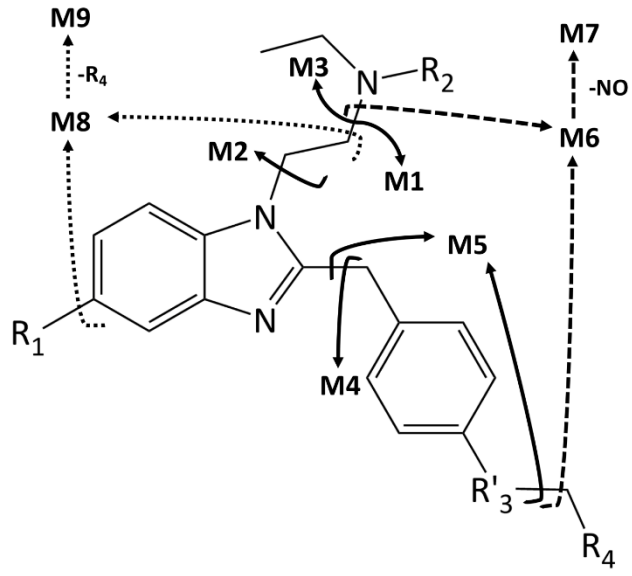

Fragment	Fragment found for
M1	3, 5, 6, 8, 9, 10, 11, 13, 14
M2	1, 2, 3, 4, 5, 6, 7, 8, 9, 10, 11, 12, 13, 14
M3	1, 3, 4, 5, 6, 8, 9, 10, 11, 12, 13, 14
M4	1, 3, 4, 5, 6, 7, 8, 9, 10, 11, 12, 13, 14
M5	1, 2, 4, 6, 7, 8, 9, 12, 14
M6	1, 7, 9, 12
M7	4
M8	3, 5, 6, 8, 10, 11
M9	1, 8, 9

Figure 4. Graphical representation of the different fragments found by liquid chromatography coupled to time-of-flight mass spectrometry (LC-QTOF-MS). Different styles of arrows were used to allow easy identification of fragmentations that result in a given fragment. In **S7**, the detailed fragmentation pathway of etonitazene can be found as an example. **S8-S24** include the fragment spectra for each compound, coupling each fragment (M1-9) to the corresponding peak.

Although even HPLC-DAD could differentiate most analogues based on absorption spectra and retention times, MS-based techniques allowed unequivocal identification and are required for identification in biological matrices. Using chromatography coupled to MS, even isomers could be distinguished based on differences in retention times and/or specific fragments. Most analogues have

very similar fragment spectra, apart from *N*-desethyl-isotonitazene and *N*-desethyl-etonitazene, which is to be expected based on their structures. Given that, for all other analogues, the fragment with *m/z* 100.11 (M2; 1,1-diethylaziridinium) is the most abundant in QTOF-MS, this fragment may be selected as a trigger for a precursor ion scan. Hence, this fragment may serve as a diagnostic marker for a specific (high-resolution) MS-based nitazene screening method. Developing highly specific targeted liquid chromatography tandem mass spectrometry (LC-MS/MS) methods should also be possible given that, for most compounds, a combination of a specific parent/fragment mass can be made.

Table 1. Summary of the analytical characterization.

	LC-QTOF-MS			GC-MS	HPLC-DAD
	RT[a] (min)	**Precursor ion (m/z)**	**Product ions (m/z) Bold: most abundant,** *italic: selective*	**Fragments (m/z)**	**Ab. max.[b] (nm)**
1. Isotonitazene	5.86	411.2436	44.05, 72.08, **100.11**, 107.05, 149.09, 250.11, 296.10	58, 86, 107	237.4 - 306.7
2. *N*-desethyl-isotonitazene	5.70	383.2095	44.05, **72.08**, 107.05, 176.05*, 224.09, 270.08, 312.13*	58, 107, 149, 325	238.4 - 305.8
3. 4'-OH-nitazene	3.94	369.1949	44.05, 72.08, **100.11**, 107.05, 250.11, 296.10	58, 86, 107*	237.8 - 305.0
4. 5-aminoisotonitazene	3.42	381.2696	44.05, 72.08, **100.11**, 107.05, 149.09, *266.13*	58, 86, 107, 380	222.7 - 273.6 - 307.6
5. Metonitazene	4.91	383.2123	44.05, 72.08, **100.11**, 121.06*, 264.13, 310.12*	58, 86, 121	237.8 - 308.5
6. Etonitazene	5.44	397.2255	44.05, 72.08, **100.11**, 107.05, 135.08*, 278.14, 324.13*	58, 86, 107, 135	238.1 - 305.8
7. *N*-desethyl-etonitazene	5.33	369.1931	44.05, **72.08**, 107.05, *135.08*, 176.05*, 252.12,* 296.10	58, 107, 135, 311*	238.8 – 306.7
8. Protonitazene	6.11	411.2466	44.05, 72.08, **100.11**, 107.05, 149.10, 250.11, *292.16, 338.15*	58, 86, 107	237.4 - 306.7
9. Butonitazene	6.69	425.2551	44.05, 72.08, **100.11**, 107.05, *163.11*, 250.11, 296.10*, 352.15*	58, 86, 107*	238.4 – 305.8
10. Clonitazene	5.57	387.1613	44.05, 72.08, **100.11**, *125.01, 268.07, 314.07*	58, 86, 125	238.4 - 305.8
11. Flunitazene	4.99	371.1890	44.05, 72.08, **100.11**, *109.04, 252.11, 298.10*	58, 86, 109	238.8 - 304.1
12. Isotodesnitazene	4.94	366.2573	44.05, 72.08, **100.11**, 107.05, 149.09, *251.11*	58, 86, 107, 365	269.6 - 276.6
13. Metodesnitazene	3.77	338.2251	44.05, 72.08, **100.11**, 121.06*,* 250.11*, 265.13*	58, 86, 121, 337	269.6 - 276.6
14. Etodesnitazene	4.43	352.2409	44.05, 72.08, **100.11**, 107.05, 135.08*, 279.15*	58, 86, 107, 135, 351	269.6 - 276.6

a, retention time; **b**, absorption maximum; *****, alternative GC-MS method was employed (cfr. Methods section).

The MOR activity of all fourteen nitazenes was evaluated using two *in vitro* recruitment assays (MOR-βarr2 and MOR-mini-Gi), generating receptor activation profiles as shown in **Figure 5. S56** provides an overlay of the MOR-βarr2 and MOR-mini-Gi recruitment profiles per compound. **Table 2** shows the derived potency (EC_{50}) and efficacy (E_{max}, relative to both fentanyl and hydromorphone) values. We found that all tested nitazenes were active at MOR, the primary molecular target for clinically applied and abused opioids.[55] Compared to other existing MOR activation assays, important features of the assays employed here include their receptor-proximal measurements, limiting signal amplification, and the use of minimally sized fusion proteins, aimed at minimally interfering with normal recruitment to the receptor.[9,56,57] In terms of potency, *N*-desethyl-isotonitazene **(2)** and etonitazene **(6)** showed the lowest EC_{50} values (i.e., the highest potencies) in both assays. These compounds were also the most efficacious in terms of both βarr2 and mini-Gi recruitment. Metodesnitazene **(13)** was the least potent compound of this panel in both bio-assays. Together with 4'-OH-nitazene **(3)**, it was also the least efficacious. Except for *N*-desethyl-isotonitazene **(2)**, the evaluated metabolites **(3, 4, 7)** were less active than their parent compounds isotonitazene **(1)** and etonitazene **(6)**. As both the EC_{50} and E_{max} values were consistently higher in the mini-Gi assay than in the βarr2 assay, the former yielded overall lower potency and higher efficacy scores.

Given that, in both assays, efficacies up to 1.4-fold that of fentanyl were found, even stronger opioid effects may be reached with most nitazenes, as compared to fentanyl. Importantly, as recently demonstrated by Gillis *et al.*, high *in vitro* efficacies may translate to a high risk of respiratory depression *in vivo.*[58,59] When considering the potency of each compound in both bio-assays (MOR-βarr2 and MOR-mini-Gi) *versus* that of fentanyl in the same respective assays, the evaluated nitazenes could be classified into roughly four categories: those with a potency around (A) 20 times higher **(2, 6)**; (B) 1.5-10 times higher **(1, 5, 7, 8)**; (C) 2-10 times lower **(9, 10, 12, 14)**; and (D) 12-50 times lower **(3, 4, 11, 13)** than that of fentanyl. In line with observations by Krotulski *et al.*[34], who noted lower isotonitazene concentrations in biological samples from fatalities than those typically found for fentanyl, it can be expected that for nitazenes from groups (A) and (B), lower doses may be sufficient to yield significant opioid effects. Although several factors (discussed further, e.g. route of administration, formation of bioactive metabolites, etc.) complicate a straightforward correlation of forensic analytical data with *in vitro* pharmacological findings, the low ng/mL blood concentrations observed in fatalities involving isotonitazene[31,34] indicate that the high MOR activity observed *in vitro* is likely paralleled by a high activity *in vivo*, suggesting that at least isotonitazene has 'suitable' pharmacokinetic properties (e.g. lipophilicity, required for brain-barrier penetration). The report of an overdose (respiratory failure and coma) following the injection of 1 mg of metonitazene **(5)** in a volunteer from an early human administration study, supports this suggestion.[23] The above further stresses the high harm potential of even small quantities of material and emphasizes the need for highly sensitive detection methods – whether analytical or activity-based.[10,60–64] In a recent report from Poland, undiluted etodesnitazene was identified in a powder. As also stated by the authors, the fact that a large amount (25.0 g) of highly pure powder was found, poses a particular threat.[44] While the exact dosage regimens for most opioids remain hard to predict (depending on e.g. existing tolerance, desired effects, pharmacokinetic properties), the relatively high potency of etodesnitazene **(14)** found in this study, further underscores this warning.

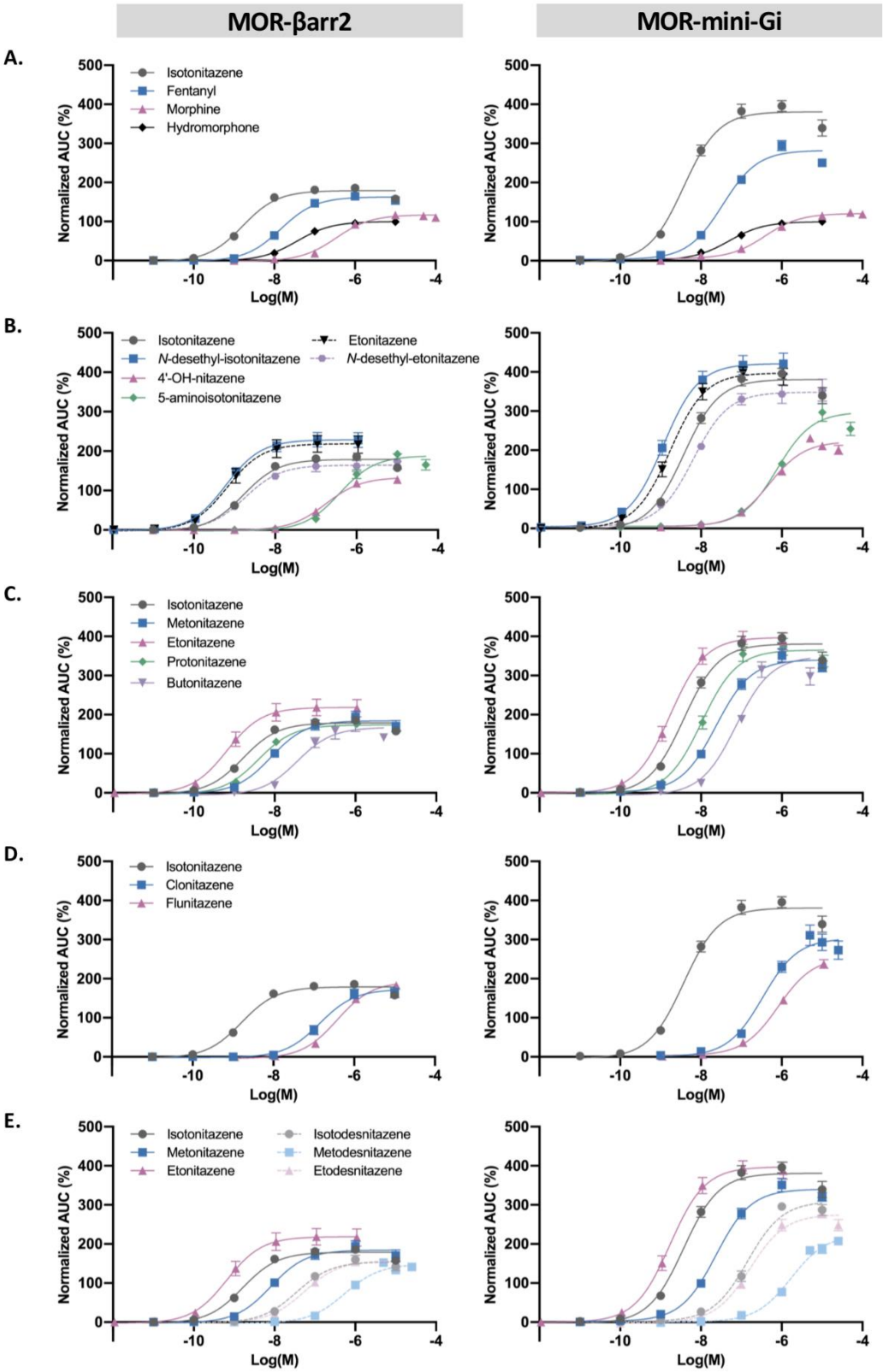

Figure 5. Activation profiles (*n*=5) obtained for isotonitazene and **(A)** fentanyl, morphine and hydromorphone; **(B)** the metabolites *N*-desethyl-isotonitazene, 4'-OH-nitazene, and 5-aminoisotonitazene, with etonitazene and *N*-desethyl-etonitazene; **(C)** metonitazene, etonitazene, protonitazene, and butonitazene; **(D)** clonitazene and flunitazene; and **(E)** the desnitazenes isotodesnitazene, metodesnitazene, etodesnitazene. The left and right panels present data from the μ-opioid receptor (MOR) β-arrestin 2 and mini-Gi recruitment assays, respectively. Data are presented as mean receptor activation ± standard error of the mean (SEM) and are normalized to the maximum response of hydromorphone.

Table 2. Overview of the potency (EC_{50}) and efficacy (E_{max}, relative to fentanyl and hydromorphone (HM)) data of the studied compounds (*n*=5). 95% confidence intervals are shown between brackets.

	MOR-βarr2			MOR-mini-Gi		
	EC_{50} (nM)	**E_{max} (% of fentanyl)**	**E_{max} (% of HM)**	**EC_{50} (nM)**	**E_{max} (% of fentanyl)**	**E_{max} (% of HM)**
1. Isotonitazene	**1.63** (1.17-2.28)	**110** (105-115)	**179** (171-187)	**3.72** (2.62-5.26)	**135** (129-141)	**381** (363-399)
2. *N*-desethyl-isotonitazene	**0.614** (0.377-0.985)	**140** (131-149)	**229** (214-243)	**1.16** (0.798-1.70)	**149** (141-157)	**421** (399-444)
3. 4'-OH-nitazene	**176** (124-250)	**81.9** (76.4-87.5)	**133** (125-143)	**486** (329-705)	**78.8** (74.2-83.6)	**223** (210-236)
4. 5-aminoisoto-nitazene	**383** (263-554)	**115** (108-123)	**188** (176-201)	**761** (505-1119)	**105** (97.3-114)	**298** (275-322)
5. Metonitazene	**8.14** (5.12-12.8)	**113** (106-121)	**184** (172-197)	**23.5** (17.7-31.4)	**121** (115-126)	**340** (326-355)
6. Etonitazene	**0.661** (0.338-1.26)	**134** (122-146)	**219** (199-238)	**1.71** (1.23-2.42)	**141** (134-148)	**397** (378-417)
7. *N*-desethyl-etonitazene	**1.81** (1.14-2.94)	**101** (94.7-107)	**164** (154-175)	**6.38** (4.64-8.67)	**123** (118-129)	**348** (333-365)
8. Protonitazene	**3.95** (2.78-5.60)	**107** (102-111)	**174** (165-182)	**10.4** (7.29-14.7)	**129** (123-136)	**365** (347-384)
9. Butonitazene	**36.2** (20.2-63.9)	**103** (92.8-113)	**167** (151-184)	**73.5** (46.9-112)	**124** (114-134)	**349** (321-378)
10. Clonitazene	**140** (93.6-210)	**106** (98.0-114)	**173** (160-187)	**338** (204-559)	**107** (100-115)	**303** (282-326)
11. Flunitazene	**377** (295-481)	**118** (113-124)	**192** (183-202)	**827** (618-1094)	**90.2** (84.7-96.0)	**255** (239-271)
12. Isotodesnitazene	**34.8** (22.1-54.4)	**94.9** (88.1-102)	**155** (144-166)	**142** (105-191)	**109** (103-116)	**309** (292-327)
13. Metodesnitazene	**548** (365-811)	**91.2** (85.1-97.5)	**149** (139-159)	**1693** (1223-2358)	**79.3** (73.9-85.4)	**224** (209-241)
14. Etodesnitazene	**54.9** (36.1-82.0)	**96.8** (90.2-103)	**158** (147-169)	**164** (119-229)	**97.6** (92.5-103)	**276** (261-290)
Morphine	**338** (239-478)	**71.9** (68.3-75.4)	**117** (111-123)	**385** (247-593)	**42.8** (40.6-45.0)	**121** (115-127)
Fentanyl	**14.4** (11.5-18.0)	***100*** *(96.5-103)*	**163** (157-169)	**34.6** (25.0-47.7)	***100*** *(94.8-105)*	**282** (268-298)
Hydromorphone	**36.2** (27.9-47.0)	**61.3** (58.9-63.8)	***100*** *(95.9-104)*	**49.3** (29.2-80.4)	**35.3** (32.7-38.1)	***100*** *(92.3-108)*

Isotonitazene was the first of the nitazenes that recently (re-)appeared on the drug market, where it has since been involved in multiple fatalities.[7,22,31–34] The exact role of isotonitazene in these deaths, however, often remains speculative.[22] Additionally, based on the results presented here, the presence of (one or more) active metabolite(s) may also contribute to the observed toxicity. We found that all three evaluated isotonitazene metabolites **(2-4)** still caused receptor activation. This is highly relevant, as these metabolites were also identified *in vivo* in human biological samples.[34] Of particular interest is the unexpected very high activity of the *N*-desethyl/nor-metabolite **(2)**. With an EC_{50} rivalling that of etonitazene – previously the most active 2-benzylbenzimidazole opioid known – the potency of this metabolite exceeds that of isotonitazene itself.[34] This likely has *in vivo* consequences, as also implied by its identification in fatalities in the US and the UK.[22,34] Interestingly, the *N*-desethyl metabolite of etonitazene **(7)**, though still being very potent, was less active than its parent compound **(6)**, indicating that *N*-dealkylation does not necessarily increase the MOR activation potential for all analogues. Reduction of the 5-nitro group of isotonitazene, a transformation that also takes place in humans,[34] results in the less active 5-amino-metabolite **(4)**. As also hypothesized by Krotulski and colleagues,[34] the 4'-OH-metabolite **(3)** is expected to be a common *in vivo* metabolite for several of the herein evaluated 2-benzylbenzimidazoles. However, with a 100-fold lower potency than isotonitazene, it is doubtful that this metabolite will significantly contribute to the overall *in vivo* effect of most analogues.[22] Interestingly, given the lower activity of **(3)** compared to most alkoxy-analogues, one could speculate that the orientation of these compounds at the MOR binding site is different from that of morphine-like compounds, in which substitution of a free phenol results in lower-affinity MOR ligands.[24,65] Considering 4'-OH-nitazene as a potential substance of abuse itself, higher doses (as compared to the main compounds) will generally be needed to obtain significant opioid effects. This matches the data from mouse studies, where a similar degree of antinociception was observed with 4'-OH-nitazene as with morphine.[13] With the caveat that it remains difficult to directly compare *in vivo* and *in vitro* results, this is roughly in line with the data presented here.

Our data show that a number of different variations to the general 2-benzylbenzimidazole structure drastically impact MOR activity. Given the increasing scheduling efforts targeting isotonitazene, a gradual shift towards the use of such analogues can be expected.[24,44] What follows is a discussion of the structure-activity relationships of 2-benzylbenzimidazoles differing from isotonitazene in the length of the alkoxy-chain **(5-9,** excl. **7)**, the type of *para*-benzyl substituent **(10, 11)** and the presence of a 5-nitro group **(12-14)**. Our *in vitro* results are discussed and compared with the findings of early *in vivo* (mouse) studies. Importantly, we cannot exclude that the activity of nitazenes at other (opioid) receptors may additionally contribute to their effects and toxicity *in vivo*. Furthermore, besides possible species differences, it should be emphasized that the eventual *in vivo* effect in humans is the result of a complex interplay of multiple factors (including route of administration, bioavailability, metabolic stability, blood-brain-barrier permeability, tolerance, ...), complicating a direct comparison with the obtained *in vitro* activity data. Nevertheless, the comparison with the well-known compounds morphine and fentanyl, as well as the implication of isotonitazene in fatalities (indicating 'suitable' pharmacokinetic properties for nitazene analogues), provides a framework that allows an estimation of the potential harmfulness of these compounds. While not specifically studied for 2-benzylbenzimidazoles, this is further supported by recent findings by Gillis *et al.,* who demonstrated that high *in vitro* MOR efficacy correlated well with respiratory depression in mice.[59]

Changing the length of the *para*-alkoxy side chain from isopropoxy **(1)** to butoxy, propoxy, ethoxy, or methoxy, respectively yields butonitazene **(9)**, protonitazene **(8)**, etonitazene **(6)**, and metonitazene

(5). Of these, the *para*-ethoxy substituent in etonitazene **(6)** yields the highest potency in both assays, followed by -isopropoxy, -propoxy, -methoxy, and -butoxy. Interestingly, this ranking matches that found in animal studies, where these compounds were compared with morphine[13,18] **(S1)**. In terms of efficacy, the E_{max} values of isoto-, meto-, proto-, and butonitazene were roughly similar, while etonitazene remained the most efficacious compound. Overall, these results indicate that either a relatively short (ethoxy) or more compact (isopropoxy) alkoxy-tail is optimal for MOR activation.

Halogenated compounds, in which the *para*-alkoxy tail is replaced by a chlorine or fluorine halogen, are represented by clonitazene **(10)** and flunitazene **(11)**, respectively. In line with *in vivo* findings,[11,13] we found that halogenation results in a drastically decreased potency, relative to isotonitazene. In a mouse tail-flick assay, clonitazene was reported to be three times more potent than morphine, while the antinociceptive potency of flunitazene was comparable to that of morphine[13] **(S1)**. This corresponds remarkably well with the *in vitro* MOR-βarr2 data reported here, where $EC_{50,morphine} \approx EC_{50,flunitazene} \approx 2.4 \times EC_{50,clonitazene}$, underscoring the possible predictive potential of our assay platform.

Desnitazenes **(12-14)** (lacking the 5-nitro group) represent the third class of benzimidazole analogues evaluated here. Animal studies previously showed that the activity of metodesnitazene approaches that of morphine. Upon further lengthening of the alkoxy-chain to etodesnitazene, the effect of morphine was exceeded about 70 times[12] **(S1)**. Again, our *in vitro* MOR-βarr2 results mirror the historic *in vivo* data, with the potency of etodesnitazene largely exceeding that of metodesnitazene and morphine. In the MOR-mini-Gi assay, metodesnitazene was up to 4 times less potent than morphine, whereas etodesnitazene remained about twice as potent. The efficacies of **(12-14)** were largely similar in the MOR-βarr2 assay, while differing slightly more in the mini-Gi assay. All three evaluated desnitazenes were generally less active than their 5-nitro counterparts **(1, 5, 6)**. Together with *in vivo* data, these results indicate an important role for the 5-nitro group in the MOR activity. This is also supported by the results for 5-aminoisotonitazene **(4)**, where reduction of the 5-nitro group led to a >200-fold reduced potency, when compared to isotonitazene.

In addition to investigating structure-activity relationships, the complementary nature of the employed bio-assays (only differing in the nature of the recruited transducer molecule, βarr2 or mini-Gi) also allowed characterization of the nitazenes in terms of potential biased agonism,[66] a recently debated subject in the field of MOR research.[56] In **Figure 6**, the bias factors (β, see Methods) for all compounds are plotted in a quantitative MOR bias plot. Compared to hydromorphone, the unbiased reference agonist (β = 0), none of the compounds evaluated in this study showed statistically significant biased agonism at MOR. This is in line with recent studies on fentanyl analogues[67] and non-fentanyl[9] opioids, in which, similarly, no bias could be detected with the assays deployed here. Given that highly similar assay platforms (monitoring activation of the serotonin 2A[68] or cannabinoid receptors[69] in lieu of MOR) have revealed statistically significant biased agonists, we consider it unlikely that the lack of significant bias observed for MOR ligands is inherent to the applied methodology. In addition, it is not clear to what extent findings related to (lack of) biased agonism can be translated to the *in vivo* situation at relevant concentrations.[70]

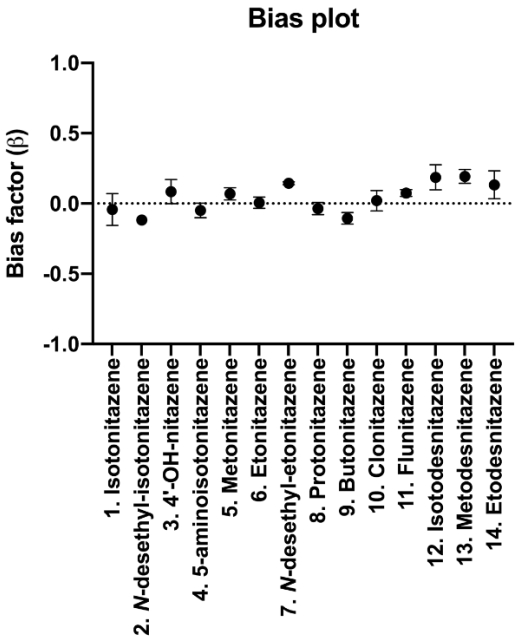

Figure 6. Quantitative μ-opioid receptor bias plot. Bias factors (β) ± SEM are plotted for all tested compounds, calculated from five independent experiments (*n*=5). Hydromorphone was used as unbiased reference agonist (β=0, not shown). Positive or negative bias factors imply a preference towards βarr2 or mini-Gi recruitment, respectively. None of the evaluated compounds showed statistically significant biased agonism at MOR, as compared to hydromorphone.

As the presence of non-fentanyl opioids on the drug market continues to rise, it will become increasingly important to rapidly identify and characterize new compounds as they emerge. Nitazenes/2-benzylbenzimidazoles are among the newest to appear and, given their high potential to activate MOR, their use poses an important risk to users. The extensive chemical and pharmacological characterization performed here may contribute to increased awareness and detection of this potentially highly dangerous class of emerging synthetic opioids.

Methods

Materials

All chemical structures of the 2-benzylbenzimidazoles/nitazenes evaluated in this study are depicted in **Figure 2** (generic scaffold) and in **S2-S4.** All concentrations are expressed as those of the free bases of the compounds. Hydromorphone was purchased as hydrochloride salt from Fagron (Nazareth, Belgium). Fentanyl was obtained as a free base from LGC Chemicals (Wesel, Germany). Morphine (free base) was acquired from Cayman Chemical Company (Ann Arbor, MI, USA). Etonitazene HCl **(6)** was procured from Chiron (Trondheim, Norway). The human embryonic kidney (HEK) 293T cells (passage 20) were kindly gifted by Prof. O. De Wever (Ghent University Hospital, Belgium). Dulbecco's Modified Eagle's Medium (DMEM; GlutaMAX™), Opti-MEM® I Reduced Serum Medium, penicillin-streptomycin (5000 U/mL) and amphotericin B (250 µg/mL) were supplied by Thermo Fisher Scientific (Pittsburg, PA, USA). Fetal bovine serum (FBS) and poly-D-lysine were purchased from Sigma-Aldrich (Overijse, Belgium). The Nano-Glo® Live Cell Assay system, containing the Nano-Glo® Live Cell Substrate and Nano-Glo® LCS Dilution Buffer, was obtained from Promega (Madison, WI, USA). All chemicals used in the generic synthesis were purchased from standard reagent suppliers such as Sigma-Aldrich (Milwaukee, WI) and were reagent-grade quality. All reagents used during the chromatographic analyses were at least of high-performance liquid chromatography (HPLC) grade.

Synthesis

The generic nitazene synthesis pathway, as outlined in the Results & Discussion section, was based on published synthesis routes, utilizing commercially available starting materials where available.[46,48] This yielded isotonitazene **(1)**, *N*-desethyl-isotonitazene HCl **(2)**, 4'-OH-nitazene **(3)**, 5-aminoisotonitazene **(4)**, metonitazene **(5)**, *N*-desethyl-etonitazene **(7)**, protonitazene HCl **(8)**, butonitazene **(9)**, clonitazene **(10)**, flunitazene HCl **(11)**, isotodesnitazene citrate **(12)**, metodesnitazene HCl **(13)** and etodesnitazene citrate **(14)**. All final products were purified to >98% HPLC-UV purity by standard purification techniques. The structure and purity of all synthesized materials was confirmed via nuclear magnetic resonance spectroscopy (^{1}H-NMR) **(S5-S6)** and extensive analytical characterization, as outlined below. ^{1}H-NMR spectra were obtained on either a Varian Unity Inova instrument (400 MHz) or a JEOL ECZ-400S (400 MHz). Samples were dissolved and recorded in DMSO-d_6.

Analytical Characterization

Analytical characterization via HPLC coupled to diode-array detection (HPLC-DAD), gas chromatography mass spectrometry (GC-MS) (except for **(3), (7)** and **(9)**) and liquid chromatography coupled to time-of-flight mass spectrometry (LC-QTOF-MS) was done as described before.[7] The details of each technique are briefly summarized below.

High-performance liquid chromatography coupled to diode array detection (HPLC-DAD)

Reversed-phase separation was performed on a LaChrom HPLC system from Merck-Hitachi (Tokyo, Japan), using a Merck Purospher® Star RP-8 endcapped column (5 µm, 125 mm x 4.6 mm) fitted with a Merck Purospher® Star RP-8 endcapped guard column (5 µm, 4 mm x 4 mm). Detection was done via DAD, monitoring a wavelength from 220 – 350 nm with a slit of 1 nm, a spectral bandwidth of 1 nm and a spectral interval of 200 msec. Concentrations of the injected dilutions ranged from 8 to 40 µg/mL.

Gas chromatography mass spectrometry (GC-MS)

One µL of a 1 mg/mL solution was injected on an Agilent 7890A GC system coupled to a 5975 XL mass-selective detector operated by MSD Chemstation software, as described in [7]. The mass spectrometer operated in SCAN-mode, scanning the range of 50 – 700 Da. For 4'-OH-nitazene **(3)**, *N*-desethyl-etonitazene **(7)**, and butonitazene **(9)**, one µL of a 1 mg/mL solution was injected on an Agilent 8890 GC system coupled to a 5977 mass-selective detector operated by OpenLabs CDS software. Injections with a split ratio of 15:1 were performed automatically at an injection temperature of 300°C, with helium as the carrier gas at a constant flow rate of 2 mL/min. A 30 m x 0.32 mm i.d. x 0.5 µm Restek Rtx-5MS column was used. For **(3)** and **(7)**, the temperature program started at 50°C for 1 min, was ramped at 30°C/min to 300°C, which was held for 16 more minutes. For **(9)**, the temperature program started at 240 °C for 1 min, was ramped at 30 °C/min to 300 °C, which was held for 27 more minutes. The transfer line temperature and ion source temperature were set at 300 and 280°C respectively. MS quadrupole temperature was set at 150 °C and an ionization energy of 70 eV was used. The mass spectrometer operated in SCAN-mode, scanning the range of 40 – 650 Da.

Liquid chromatography coupled to time-of-flight mass spectrometry (LC-QTOF-MS)

Using a 1 µg/mL solution, spectra were recorded after infusion or after chromatographic separation. The latter was accomplished with an Agilent 1290 Infinity LC system and a Phenomenex Kinetex C18-column (2.6 µm, 3 x 50 mm), maintained at 30°C. The high-resolution mass spectrometry system was a 5600+ QTOF from Sciex, with an electrospray ionization (ESI) source and Analyst TF 1.7.1 software, from the same provider. Settings for QTOF-MS were the same as published before.[7] The LC-QTOF-MS settings resulted in TOF-MS full scan spectra combined with data dependent acquisition of product ion spectra (both scanning from 5 to 450 Da).

Determination of *in vitro* biological activity at the µ-opioid receptor (MOR)

Cell culture

HEK 293T cells stably expressing either the MOR-βarr2-GRK2 or MOR-mini-Gi system (see below) were routinely maintained in DMEM (GlutaMAX™) supplemented with 10% heat-inactivated FBS, 100 IU/mL penicillin, 100 mg/L streptomycin and 0.25 mg/L amphotericin B. The cells were cultured at 37°C in a humidified atmosphere containing 5% CO_2. The stability of the cell lines was routinely monitored via flow cytometric analysis of co-expressed markers.[67]

NanoBiT MOR-β-arrestin2/mini-Gi recruitment bio-assay

Two stable cell-based reporter assays were used to assess the *in vitro* biological MOR activity of fourteen different nitazenes, fentanyl, morphine and hydromorphone. The employed assays have been described before.[63,67] In short, activation of human MOR, fused to one part of a split nanoluciferase (NanoLuc® Binary Technology, Promega), results in the recruitment of either β-arrestin2 (βarr2) (in the presence of co-expressed G protein-coupled receptor kinase 2, GRK2) or mini-Gi (GTPase domain of the Gαi subunit), fused to the complementing part of the split nanoluciferase. The resulting functional complementation of the nanoluciferase restores its enzymatic activity, which, upon addition of the substrate furimazine, yields a measurable bioluminescent signal.

Cells expressing either MOR-βarr2-GRK2 (for simplicity, referred to as MOR-βarr2) or MOR-mini-Gi were seeded on poly-D-lysine coated 96-well plates (5 x 10^4 cells/well) one day prior to the experiments. Following overnight incubation, the cells were washed twice with Opti-MEM® I Reduced Serum Medium before adding 90 µL OptiMEM®. Nano-Glo® Live Cell reagent was then prepared by 20-fold dilution of Nano-Glo® Live Cell Substrate with Nano-Glo® LCS Dilution Buffer, and 25 µL was added to each well. The plate was subsequently placed into a TriStar^2 LB 942 multimode microplate reader (Berthold Technologies GmbH & Co., Bad Wildbad, Germany) and luminescence was continuously monitored until stabilization of the signal (10-15 minutes). Next, 20 µL of a 6.75-fold concentrated stock solution of each test compound (in Opti-MEM®/MeOH or Opti-MEM®/ACN) was added per well and luminescence was monitored for 2 hours. All compounds were tested in both assays in concentrations ranging between 1 pM and 100 µM, with appropriate solvent controls included in each experiment. Each compound was evaluated in five independent experiments (*n*=5), with duplicates run for each concentration within an experiment to ensure the reliability of single values.

Data and statistical analysis

Absolute time-luminescence profiles obtained during the two-hour read-out were corrected for inter-well variability and used for calculation of the area under the curve (AUC), as previously detailed by Pottie *et al.*[71] Solvent controls were performed by subtraction of the mean AUC of the corresponding blank. Concentration-response curves were subsequently generated via GraphPad Prism 8 software (San Diego, CA, USA) via three-parametric nonlinear regression, which implies a fixed Hill slope of 1. The use of this model is required for the implementation of the ligand bias calculation described below.[72,73] To facilitate interpretation and comparison between different studies, the data were normalized to the maximum response of hydromorphone (arbitrarily set at 100%) for each experiment. Hydromorphone was selected as a reference agonist for normalization based on previous experience.[7–10,67] To facilitate interpretation of the data, efficacies were also calculated relative to fentanyl. A part of the data for fentanyl (*n*=3 out of the total of *n*=5 experiments) were also reported in Vandeputte *et al.*[9] Morphine was included for comparison, further facilitating interpretation of the data. It was defined *a priori* that AUC values from the highest concentration(s) were excluded in case of a reduction of 20% or more compared to the AUC of the next dilution. As previously hypothesized for different receptor systems,[9,68] high concentrations may potentially lead to cell toxicity or solubility issues, with a rapid drop of the signal resulting in a lower AUC. Inclusion of such data points could inadvertently skew the obtained concentration-response graph. Using the standard Grubbs' test, the complete dataset (2349 data points) was screened for outliers, resulting in a total of 17 outliers (0.72%) that were subsequently omitted from the data set. All duplicate data points were considered separately in the Grubbs' test. This means that data points were only excluded if a single value (out of e.g. *n* = 5 x 2) was considered an outlier in the Grubbs' test, as in this case the reliability of this single value could not be ensured. For each compound, the normalized data from five separate experiments were then combined to obtain final EC_{50} and E_{max} values, which are measures of respectively potency and efficacy (the latter relative to hydromorphone or fentanyl).

Pathway bias was calculated as previously described.[68,73] In line with previous studies, hydromorphone was employed as reference agonist that is considered unbiased.[9,67] To avoid refitting of the concentration-response data to a more complex model, bias was calculated via the intrinsic relative activity scale (RA_i), a validated alternative to the Black & Leff operational model.[74–76] An important advantage of using the Ra_i is that it can be calculated almost directly from EC_{50} and E_{max} values as

observable from the concentration-response curves with a Hill slope fixed at 1. First, the RA_i was calculated for each compound in both bioassays (Equation 1; *i* = test compound and HM = unbiased reference agonist, hydromorphone):[77,78]

$$RA_{i,reference\ agonist}^{pathway} = \frac{\frac{E_{max,i}}{EC_{50,i}}}{\frac{E_{max,HM}}{EC_{50,HM}}} = \frac{EC_{50,HM}\ x\ E_{max,i}}{E_{max,HM}\ x\ EC_{50,i}}$$

The obtained RA_i values per pathway were then combined into a bias factor (β_i) for each individual compound according to Equation 2:[72,73]

$$\beta_i = \log(\frac{RA_{i,HM}^{\beta arr2}}{RA_{i,HM}^{mini-Gi}})$$

Compared to the reference hydromorphone (β = 0, as it is considered unbiased), compounds with a positive value for β tend to favor βarr2 recruitment, whereas a bias factor below zero indicates a certain extent of bias towards mini-Gi recruitment. The bias factor for each compound was calculated from five independent experiments, each performed in duplicate. Statistical analysis was carried out in GraphPad Prism 8 by non-parametric one-way ANOVA (Kruskal-Wallis), followed by a post hoc Dunn's test. Differences were considered statistically significant when $p < 0.05$.

Author contributions

N.K., D.St.G., and D.I. synthesized all compounds and performed ^{1}H-NMR. M.V. executed the *in vitro* functional assays and K.V.U. performed the analytical characterization, both under the supervision of C.S. M.V., K.V.U., and C.S. conceived the experiments and wrote the manuscript, and all authors reviewed and edited drafts of the manuscript. All authors approved the final version of the paper.

Funding sources

This work was supported by the Research Foundation-Flanders (FWO) (grant no. 3S038719 to M.V.) and the Ghent University Special Research Fund (BOF) (grant no. 01J15517 to C.S.).

Conflict of interest

The authors declare no conflicts of interest.

Acknowledgments

We gratefully acknowledge Chiron for the gifting of etonitazene. The knowledgeable lab technicians of the Laboratory of Toxicology are acknowledged for performing part of the experiments for the analytical characterization.

Supporting information

S1, Summary of Data from Early Swiss Literature; S2-S4, Overview substances; S5-S6, ^{1}H-NMR; S7, Detailed fragmentation (QTOF-MS); S8-S24, LC-QTOF-MS; S25-S39, GC-MS; S40-S55, HPLC-DAD; S56, Overlay β-arrestin 2 *vs.* mini-Gi data.

References

(1) UNODC. *World Drug Report 2020*; E.20.XI.6; United Nations publication: Vienna, Austria, 2020; Vol. E.20.XI.6.

(2) UNODC. *The Growing Complexity of the Opioid Crisis. Global SMART Update, Volume 24*; Global SMART Update; Vienna, 2020.

(3) EMCDDA. *European Drug Report 2020: Trends and Developments*; Publications Office of the European Union: Luxembourg, 2020.

(4) Bao, Y.; Meng, S.; Shi, J.; Lu, L. Control of Fentanyl-Related Substances in China. *The Lancet Psychiatry* **2019**, *6* (7), e15. https://doi.org/10.1016/S2215-0366(19)30218-4.

(5) Belgisch Staatsblad. *Koninklijk Besluit Houdende Regeling van Verdovende Middelen, Psychotrope Stoffen (Federale Overheidsdienst Volksgezondheid Veiligheid van de Voedselketen En Leefmilieu)*; 2017.

(6) 116th Congress. *S.3201 - Temporary Reauthorization and Study of the Emergency Scheduling of Fentanyl Analogues Act*; 2020.

(7) Blanckaert, P.; Cannaert, A.; Van Uytfanghe, K.; Hulpia, F.; Deconinck, E.; Van Calenbergh, S.; Stove, C. P. Report on a Novel Emerging Class of Highly Potent Benzimidazole NPS Opioids: Chemical and in Vitro Functional Characterization of Isotonitazene. *Drug Testing and Analysis* **2020**, *12*, 422–430. https://doi.org/10.1002/dta.2738.

(8) Cannaert, A.; Hulpia, F.; Risseeuw, M.; Van Uytfanghe, K.; Deconinck, E.; Van Calenbergh, S.; Blanckaert, P.; Stove, C. P. Report on a New Opioid NPS: Chemical and in Vitro Functional Characterization of a Structural Isomer of the MT-45 Derivative Diphenpipenol. *Journal of Analytical Toxicology* **2020**, bkaa066. https://doi.org/10.1093/jat/bkaa066.

(9) Vandeputte, M. M.; Cannaert, A.; Stove, C. P. In Vitro Functional Characterization of a Panel of Non-Fentanyl Opioid New Psychoactive Substances. *Archives of Toxicology* **2020**, *94(11)*, 3819–3830. https://doi.org/10.1007/s00204-020-02855-7.

(10) Verougstraete, N.; Vandeputte, M. M.; Lyphout, C.; Cannaert, A.; Hulpia, F.; Van Calenbergh, S.; Verstraete, A. G.; Stove, C. P. First Report on Brorphine: The next Opioid on the Deadly New Psychoactive Substances' Horizon? *Journal of Analytical Toxicology* **2020**, *44* (9), 937–946. https://doi.org/10.1093/jat/bkaa094.

(11) Hunger, A.; Kebrle, J.; Rossi, A.; Hoffmann, K. Synthese basisch substituierter, analgetisch wirksamer Benzimidazol-Derivate. *Experientia* **1957**, *13* (10), 400–401. https://doi.org/10.1007/BF02161116.

(12) Hunger, A.; Kebrle, J.; Rossi, A.; Hoffmann, K. Benzimidazol-Derivate und verwandte Heterocyclen II. Synthese von 1-Aminoalkyl-2-benzyl-benzimidazolen. *Helvetica Chimica Acta* **1960**, *43* (3), 800–809. https://doi.org/10.1002/hlca.19600430323.

(13) Hunger, A.; Kebrle, J.; Rossi, A.; Hoffmann, K. Benzimidazol-Derivate und verwandte Heterocyclen III. Synthese von 1-Aminoalkyl-2-benzyl-nitro-benzimidazolen. *Helvetica Chimica Acta* **1960**, *43* (4), 1032–1046. https://doi.org/10.1002/hlca.19600430412.

(14) Hunger, A.; Kebrle, J.; Rossi, A.; Hoffmann, K. Benzimidazol-Derivate Und Verwandte Heterocyclen VI. Synthese von Phenyl-[1-Aminoalkyl-Benzimidazolyl-(2)]-Essigsäure-Estern Und -Amiden. *Helvetica Chimica Acta* **1960**, *43* (6), 1727–1733. https://doi.org/10.1002/hlca.19600430634.

(15) Hunger, A.; Kebrle, J.; Rossi, A.; Hoffmann, K. Benzimidazol-Derivate und verwandte Heterocyclen VII. Synthese neuer 2-Amino-benzimidazole. *Helvetica Chimica Acta* **1961**, *44* (5), 1273–1282. https://doi.org/10.1002/hlca.19610440513.

(16) Rossi, A.; Hunger, A.; Kebrle, J.; Hoffmann, K. Benzimidazol-Derivate und verwandte Heterocyclen IV. Die Kondensation von o-Phenylendiamin mit α-Aryl- und γ-Aryl-acetessigester. *Helvetica Chimica Acta* **1960**, *43* (4), 1046–1056. https://doi.org/10.1002/hlca.19600430413.

(17) Rossi, A.; Hunger, A.; Kebrle, J.; Hoffmann, K. Benzimidazol-Derivate und verwandte Heterocyclen V. Die Kondensation von o-Phenylendiamin mit aliphatischen und alicyclischen β-Ketoestern. *Helvetica Chimica Acta* **1960**, *43* (5), 1298–1313. https://doi.org/10.1002/hlca.19600430515.

(18) Gross, F.; Turrian, H. Über Benzimidazolderivate mit starker analgetischer Wirkung. *Experientia* **1957**, *13* (10), 401–403. https://doi.org/10.1007/BF02161117.

(19) Hoffmann, K.; Hunger, A.; Kebrle, J.; Rossi, A. Verfahren Zur Herstellung Analgetisch Wirksamer Benzimidazole. DE Patent 1057123B, 1959.

(20) Hoffmann, K.; Hunger, A.; Rossi, A. Benzimidazoles. US patent 2935514A, 1960.

(21) Hoffmann, K.; Hunger, A.; Kebrle, J.; Rossi, A. Verfahren Zur Herstellung Neuer Benzimidazole. CH Patent 362080A, 1962.

(22) EMCDDA. *Report on the Risk Assessment of N,N-Diethyl-2- [[4-(1-Methylethoxy)Phenyl]Methyl]-5-Nitro-1Hbenzimidazole- 1-Ethanamine (Isotonitazene) in Accordance with Article 5c of Regulation (EC) No 1920/2006 (as Amended)*; Publications Office: Luxembourg, 2020.

(23) Bromig, G. Über Neue Starkwirkende Analgetika Und Ihre Klinische Erprobung. *Klinische Wochenschrift* **1958**, *36* (20), 960–963. https://doi.org/10.1007/BF01486702.

(24) Ujváry, I.; Christie, R.; Evans-Brown, M.; Gallegos, A.; Jorge, R.; de Morais, J.; Sedefov, R. DARK Classics in Chemical Neuroscience: Etonitazene and Related Benzimidazoles. *ACS Chemical Neuroscience*.

(25) Shulgin, A. T. Drugs of Abuse in the Future. *Clinical Toxicology* **1975**, *8* (4), 405–456. https://doi.org/10.3109/15563657508990076.

(26) Brandenberger, H. Die Rolle Des Massenspektrometers Im Toxikologisch-Chemischen Laboratorium. *Deutsche Lebensmittel-Rundschau* **1974**, *70(1)*, 31–39.

(27) Morris, H. Synthetic opioids: the most addictive drugs in the world https://www.vice.com/en/article/9bdymy/hamiltons-pharmacopeia-804-v16n4 (accessed Oct 26, 2020).

(28) Reavy, P. Utah case of potent drug is U.S. first https://www.deseret.com/2003/6/3/19726293/utah-case-of-potent-drug-is-u-s-first (accessed Oct 26, 2020).

(29) Sorokin, V. I. Illegal Synthesis of Etonitazene. *Journal of the Clandestine Laboratory Investigating Chemists Association* **1999**, *9* (2–3), 20.

(30) Sorokin, V. I.; Ponkratov, K. V.; Drozdov, M. A. Etonitazene Encountered in Moscow. *Microgram* **1999**, *32* (9), 239–244.

(31) Mueller, F.; Bogdal, C.; Pfeiffer, B.; Andrello, L.; Ceschi, A.; Thomas, A.; Grata, E. Isotonitazene: Fatal Intoxication in Three Cases Involving This Unreported Novel Psychoactive Substance in Switzerland. *Forensic Science International* **2021**, *320*, 110686. https://doi.org/10.1016/j.forsciint.2021.110686.

(32) Krotulski, A. J.; Logan, B. K. Isotonitazene https://www.npsdiscovery.org/wp-content/uploads/2019/11/Isotonitazene_112119_ToxicologyAnalyticalReport.pdf (accessed Mar 10, 2020).

(33) Krotulski, A. J.; Papsun, D. M.; Fogarty, M. F.; Nelson, L.; Logan, B. K. Potent synthetic opioid - isotonitazene - recently identified in the Midwestern United States https://www.npsdiscovery.org/wp-content/uploads/2019/11/Public-Alert_Isotonitazene_NPS-Discovery_111919-1.pdf (accessed Dec 1, 2019).

(34) Krotulski, A. J.; Papsun, D. M.; Kacinko, S. L.; Logan, B. K. Isotonitazene Quantitation and Metabolite Discovery in Authentic Forensic Casework. *Journal of Analytical Toxicology* **2020**, *44* (6), 521–530. https://doi.org/10.1093/jat/bkaa016.

(35) Mohr, A. L.; Salas, J. R.; Logan, B. K. Toxicological Time Travel: Retrospective Datamining of Analytical Time-of-Flight Mass Spectrometry (TOFMS) Data for Evaluating the Rise and Fall of Novel Opioid and Fentanyl Analog Use in the United States. **2020**.

(36) DEA. *21 CFR Part 1308. Schedules of Controlled Substances: Temporary Placement of Isotonitazene in Schedule I*; 2020.

(37) DEA. *21 CFR Part 1300.01 Definitions Relating to Controlled Substances*.

(38) European Commission. *Commission Delegated Directive (EU) 2020/1687 of 2 September 2020 Amending the Annex to Council Framework Decision 2004/757/JHA as Regards the Inclusion of the New Psychoactive Substance N,N-Diethyl-2-[[4-(1-Methylethoxy)Phenyl]Methyl]-5-Nitro-1H-Benzimidazole-1-Ethanamine (Isotonitazene) in the Definition of 'Drug';* 2020.

(39) UNODC. *The International Drug Control Conventions: Schedules of the Single Convention on Narcotic Drugs of 1961, as Amended by the 1972 Protocol, as at 22 January 2021*; 2021.

(40) WHO. 43rd ECDD (2020): Critical review report: isotonitazene https://www.who.int/docs/default-source/controlled-substances/43rd-ecdd/isonitazene-43rd-final-complete-a.pdf (accessed Feb 1, 2021).

(41) Krotulski, A. J.; Shuda, S. A.; Fogarty, M. F.; Decker, S. E.; Logan, B. K. Metonitazene https://www.npsdiscovery.org/wp-content/uploads/2020/07/Metonitazene_073020_NMSLabs_Report.pdf (accessed Jul 30, 2020).

(42) Krotulski, A. J.; Papsun, D. M.; Walton, S. E.; Logan, B. K. Public alert: Metonitazene begins proliferation as newest synthetic opioid among latest cycle of non-fentanyl related drugs https://www.npsdiscovery.org/wp-content/uploads/2021/01/Public-Alert_Metonitazene_NPS-Discovery_012521.pdf (accessed Feb 1, 2021).

(43) Krotulski, A. J.; Perch, S.; Walton, S. E.; Fogarty, M. F.; Papsun, D. M.; Logan, B. K. Butonitazene https://www.npsdiscovery.org/wp-content/uploads/2021/01/Butonitazene_011521_ToxicologyAnalyticalReport.pdf (accessed Feb 25, 2021).

(44) Siczek, M.; Zawadzki, M.; Siczek, M.; Chłopaś-Konowałek, A.; Szpot, P. Etazene (*N,N*-Diethyl-2-{[(4-Ethoxyphenyl)Methyl]-1*H*-Benzimidazol-1-Yl}-Ethan-1-Amine (Dihydrochloride)): A Novel Benzimidazole Opioid NPS Identified in Seized Material: Crystal Structure and Spectroscopic Characterization. *Forensic Toxicology* **2021**, *39*, 146–155. https://doi.org/10.1007/s11419-020-00552-9.

(45) Schultz, J.; Raje, S.; Short, S.; Stauffenberg, M.; Krotulski, A. J.; Fogarty, M. F.; Logan, B. K. Etodesnitazene https://www.npsdiscovery.org/wp-content/uploads/2021/02/Etodesnitazene_022321_ToxicologyAnalyticalReport.pdf (accessed Feb 24, 2021).

(46) Carroll, F. I.; Coleman, M. C. Etonitazene. An Improved Synthesis. *Journal of Medicinal Chemistry* **1975**, *18* (3), 318–320. https://doi.org/10.1021/jm00237a024.

(47) Kim, Y.; Kumar, M. R.; Park, N.; Heo, Y.; Lee, S. Copper-Catalyzed, One-Pot, Three-Component Synthesis of Benzimidazoles by Condensation and C–N Bond Formation. *The Journal of Organic Chemistry* **2011**, *76* (23), 9577–9583. https://doi.org/10.1021/jo2019416.

(48) Renton, P.; Green, B.; Maddaford, S.; Rakhit, S.; Andrews, J. S. NOpiates: Novel Dual Action Neuronal Nitric Oxide Synthase Inhibitors with μ-Opioid Agonist Activity. *ACS Medicinal Chemistry Letters* **2012**, *3* (3), 227–231. https://doi.org/10.1021/ml200268w.

(49) Thomas, J. B.; Fall, M. J.; Cooper, J. B.; Burgess, J. P.; Carroll, F. I. Rapid In-Plate Generation of Benzimidazole Libraries and Amide Formation Using EEDQ. *Tetrahedron letters* **1997**, *38* (29), 5099–5102. https://doi.org/10.1016/S0040-4039(97)01136-2.

(50) Bucha, M.; Eppakayala, L.; Maringanti, T. C. A Facile Synthesis and Molecular Docking for Anti-Inflammatory Activity of 2-(4-Chlorobenzyl)-1-(2-(Pyrrolidin-1-Yl)Ethyl)-1H-Benzo[d]Imidazol-5-Amine and 2-(4- Chlorobenzyl)-1-((1-Ethylpyrrolidin-2-Yl)Methyl)-1H-Benzo[d]Imidazol-5-Amine. *J. Heterocycl. Chem.* **2018**, *4*, 321–327.

(51) Porter, H. K. The Zinin Reduction of Nitroarenes. In *Organic Reactions*; John Wiley & Sons, Inc., Ed.; John Wiley & Sons, Inc.: Hoboken, NJ, USA, 2011; pp 455–481. https://doi.org/10.1002/0471264180.or020.04.

(52) Weissberg, A.; Madmon, M.; Dagan, S. Structural Identification of Compounds Containing Tertiary Amine Side Chains Using ESI-MS3 Combined with Fragmentation Pattern Matching to Chemical Analogues – Benzimidazole Derivatives as a Case Study. *International Journal of Mass Spectrometry* **2016**, *394*, 9–21. https://doi.org/10.1016/j.ijms.2015.11.002.

(53) Cayman Chemical Company. Nitazenes https://www.caymanchem.com/search?q=nitazene (accessed Oct 28, 2020).

(54) Shamai Yamin, T.; Prihed, H.; Shifrovitch, A.; Dagan, S.; Weissberg, A. Oxidation-Assisted Structural Elucidation of Compounds Containing a Tertiary Amine Side Chain Using Liquid Chromatography Mass Spectrometry. *Journal of Mass Spectrometry* **2018**, *53* (6), 518–524. https://doi.org/10.1002/jms.4081.

(55) Charbogne, P.; Kieffer, B. L.; Befort, K. 15 Years of Genetic Approaches in Vivo for Addiction Research: Opioid Receptor and Peptide Gene Knockout in Mouse Models of Drug Abuse. *Neuropharmacology* **2014**, *76*, 204–217. https://doi.org/10.1016/j.neuropharm.2013.08.028.

(56) Gillis, A.; Kliewer, A.; Kelly, E.; Henderson, G.; Christie, M. J.; Schulz, S.; Canals, M. Critical Assessment of G Protein-Biased Agonism at the μ-Opioid Receptor. *Trends in Pharmacological Sciences* **2020**, *41* (12), 947–959. https://doi.org/10.1016/j.tips.2020.09.009.

(57) Wouters, E.; Walraed, J.; Banister, S. D.; Stove, C. P. Insights into Biased Signaling at Cannabinoid Receptors: Synthetic Cannabinoid Receptor Agonists. *Biochemical Pharmacology* **2019**, *169*, 113623. https://doi.org/10.1016/j.bcp.2019.08.025.

(58) Benredjem, B.; Gallion, J.; Pelletier, D.; Dallaire, P.; Charbonneau, J.; Cawkill, D.; Nagi, K.; Gosink, M.; Lukasheva, V.; Jenkinson, S.; Ren, Y.; Somps, C.; Murat, B.; Van Der Westhuizen, E.; Le Gouill, C.; Lichtarge, O.; Schmidt, A.; Bouvier, M.; Pineyro, G. Exploring Use of Unsupervised Clustering to Associate Signaling Profiles of GPCR Ligands to Clinical Response. *Nat Commun* **2019**, *10* (1), 4075. https://doi.org/10.1038/s41467-019-11875-6.

(59) Gillis, A.; Gondin, A. B.; Kliewer, A.; Sanchez, J.; Lim, H. D.; Alamein, C.; Manandhar, P.; Santiago, M.; Fritzwanker, S.; Schmidel, F.; Katte, T. A.; Reekie, T.; Grimsey, N. L.; Kassiou, M.; Kellam, B.; Krasel, C.; Halls, M. L.; Connor, M.; Lane, J. R.; Schulz, S.; Christie, M. J.; Canals, M. Low Intrinsic Efficacy for G Protein Activation Can Explain the Improved Side Effect Profiles of New Opioid Agonists. *Sci. Signal.* **2020**, *13* (625), eaaz3140. https://doi.org/10.1126/scisignal.aaz3140.

(60) Cannaert, A.; Vasudevan, L.; Friscia, M.; Mohr, A. L. A.; Wille, S. M. R.; Stove, C. P. Activity-Based Concept to Screen Biological Matrices for Opiates and (Synthetic) Opioids. *Clinical Chemistry* **2018**, *64* (8), 1221–1229. https://doi.org/10.1373/clinchem.2018.289496.

(61) Cannaert, A.; Storme, J.; Hess, C.; Auwärter, V.; Wille, S. M. R.; Stove, C. P. Activity-Based Detection of Cannabinoids in Serum and Plasma Samples. *Clinical Chemistry* **2018**, *64* (6), 918–926. https://doi.org/10.1373/clinchem.2017.285361.

(62) Cannaert, A.; Vandeputte, M. M.; Wille, S. M. R.; Stove, C. P. Activity-Based Reporter Assays for the Screening of Abused Substances in Biological Matrices. *Critical Reviews in Toxicology* **2019**, *49* (2), 95–109. https://doi.org/10.1080/10408444.2019.1576588.

(63) Cannaert, A.; Deventer, M.; Fogarty, M.; Mohr, A. L. A.; Stove, C. P. Hide and Seek: Overcoming the Masking Effect of Opioid Antagonists in Activity-Based Screening Tests. *Clinical Chemistry* **2019**, *65* (12), 1604–1605. https://doi.org/10.1373/clinchem.2019.309443.

(64) Cannaert, A.; Vandeputte, M. M.; Hudson, S.; Wood, D. M.; Dargan, P. I.; Stove, C. P. Validation of Activity-Based Screening for Synthetic Cannabinoid Receptor Agonists in a Large Set of Serum Samples. *Clinical Chemistry* **2019**, *65* (2), 347–349. https://doi.org/10.1373/clinchem.2018.296905.

(65) Devereaux, A. L.; Mercer, S. L.; Cunningham, C. W. DARK Classics in Chemical Neuroscience: Morphine. *ACS Chem. Neurosci.* **2018**, *9* (10), 2395–2407. https://doi.org/10.1021/acschemneuro.8b00150.

(66) Wootten, D.; Christopoulos, A.; Marti-Solano, M.; Babu, M. M.; Sexton, P. M. Mechanisms of Signalling and Biased Agonism in G Protein-Coupled Receptors. *Nature Reviews Molecular Cell Biology* **2018**, *19* (10), 638–653. https://doi.org/10.1038/s41580-018-0049-3.

(67) Vasudevan, L.; Vandeputte, M. M.; Deventer, M.; Wouters, E.; Cannaert, A.; Stove, C. P. Assessment of Structure-Activity Relationships and Biased Agonism at the Mu Opioid Receptor of Novel Synthetic Opioids Using a Novel, Stable Bio-Assay Platform. *Biochemical Pharmacology* **2020**, *177*, 113910. https://doi.org/10.1016/j.bcp.2020.113910.

(68) Pottie, E.; Dedecker, P.; Stove, C. P. Identification of Psychedelic New Psychoactive Substances (NPS) Showing Biased Agonism at the 5-HT_{2A}R through Simultaneous Use of β-Arrestin 2 and Mini$G_{\alpha q}$ Bioassays. *Biochemical Pharmacology* **2020**, 114251. https://doi.org/10.1016/j.bcp.2020.114251.

(69) Wouters, E.; Walraed, J.; Robertson, M. J.; Meyrath, M.; Szpakowska, M.; Chevigné, A.; Skiniotis, G.; Stove, C. Assessment of Biased Agonism among Distinct Synthetic Cannabinoid Receptor Agonist Scaffolds. *ACS Pharmacol. Transl. Sci.* **2020**, *3* (2), 285–295. https://doi.org/10.1021/acsptsci.9b00069.

(70) Luttrell, L. M.; Maudsley, S.; Bohn, L. M. Fulfilling the Promise of "Biased" G Protein–Coupled Receptor Agonism. *Mol Pharmacol* **2015**, *88* (3), 579–588. https://doi.org/10.1124/mol.115.099630.

(71) Pottie, E.; Tosh, D. K.; Gao, Z.-G.; Jacobson, K. A.; Stove, C. P. Assessment of Biased Agonism at the A_3 Adenosine Receptor Using β-Arrestin and Mini$G_{\alpha i}$ Recruitment Assays. *Biochemical Pharmacology* **2020**, *177*, 113934. https://doi.org/10.1016/j.bcp.2020.113934.

(72) Ehlert, F. J. On the Analysis of Ligand-Directed Signaling at G Protein-Coupled Receptors. *Naunyn-Schmiedeberg's archives of pharmacology* **2008**, *377* (4–6), 549–577. https://doi.org/10.1007/s00210-008-0260-4.

(73) Rajagopal, S.; Ahn, S.; Rominger, D. H.; Gowen-MacDonald, W.; Lam, C. M.; DeWire, S. M.; Violin, J. D.; Lefkowitz, R. J. Quantifying Ligand Bias at Seven-Transmembrane Receptors. *Molecular Pharmacology* **2011**, *80* (3), 367–377. https://doi.org/10.1124/mol.111.072801.

(74) Black, J. W.; Leff, P. Operational Models of Pharmacological Agonism. *Proceedings of the Royal Society of London - Biological Sciences* **1983**, *220* (1219), 141–162. https://doi.org/10.1098/rspb.1983.0093.

(75) Gillis, A.; Sreenivasan, V.; Christie, M. J. Intrinsic Efficacy of Opioid Ligands and Its Importance for Apparent Bias, Operational Analysis, and Therapeutic Window. *Mol Pharmacol* **2020**, *98* (4), 410–424. https://doi.org/10.1124/mol.119.119214.

(76) Winpenny, D.; Clark, M.; Cawkill, D. Biased Ligand Quantification in Drug Discovery: From Theory to High Throughput Screening to Identify New Biased μ Opioid Receptor Agonists: Identification of New Biased μ Receptor Agonists. *British Journal of Pharmacology* **2016**, *173* (8), 1393–1403. https://doi.org/10.1111/bph.13441.

(77) Ehlert, F. J.; Griffin, M. T.; Sawyer, G. W.; Bailon, R. A Simple Method for Estimation of Agonist Activity at Receptor Subtypes: Comparison of Native and Cloned M_3 Muscarinic Receptors in Guinea Pig Ileum and Transfected Cells. *The Journal of Pharmacology and Experimental Therapeutics* **1999**, *289* (2), 981–992.

(78) Griffin, M. T.; Figueroa, K. W.; Liller, S.; Ehlert, F. J. Estimation of Agonist Activity at G Protein-Coupled Receptors: Analysis of M_2 Muscarinic Receptor Signaling through $G_{i/o}$, G_s, and G_{15}. *J Pharmacol Exp Ther* **2007**, *321* (3), 1193–1207. https://doi.org/10.1124/jpet.107.120857.

For Table of Contents only